

Chirality-Induced Spin Filtering in Pseudo Jahn-Teller Molecules

Akihito Kato,¹ Hiroshi M. Yamamoto,² and Jun-ichiro Kishine^{1,2}

¹*Division of Natural and Environmental Sciences, The Open University of Japan, Chiba 261-8586, Japan*

²*Research Center of Integrative Molecular Systems, Institute for Molecular Science, Okazaki, Aichi 444-8585, Japan*

(Dated: November 29, 2021)

Chirality-induced spin selectivity (CISS) refers to an ability to induce a spin polarization of an electron transmitted through chiral materials. An important experimental observation is that incredibly large spin polarization is realized at room temperature even for the organic molecules that have weak spin-orbit coupling (SOC), although SOC is an only interaction that can manipulate the electrons' spins in the setups. Therefore, the mechanism of the CISS needs to be constructed in a way insensitive to or enhancing the magnitude of the SOC strength. In this Letter, we describe a theoretical study for CISS with a model chiral molecule that belongs to the point group C_3 . In this molecule, electronic translational and rotational degrees of freedom for an injected electron are coupled one another via the nuclear vibrational mode with a pseudo Jahn-Teller effect. By properly taking the molecular symmetry as well as the time reversal symmetry into account and classifying the molecular ground states by their angular and spin momentum quantum numbers, we show that the chiral molecule can act as an efficient spin-filter. The efficiency of this spin-filtering can be nearly independent of the SOC strength in this model, while it well exceeds the spin-polarization relying solely on the SOC. The nuclear vibrations turned out to have the role of not only mediating the translation-rotation coupling, but also enhancing the spin-filtering efficiency.

Introduction. An object that cannot be overlapped with its mirror images, namely, that lacks the reflection symmetries, is called chiral. The chiral symmetry breaking gives rise to abundant functionality [1] such as chiral magnetism [2, 3], chiral phononics [4–6], chiral photonics [7], and nonreciprocal conductivity [8, 9]. Recent experimental observations have confirmed that the chiral materials exhibit spin-selective phenomena, including a large spin-polarization of photoelectrons transmitted through helical molecules [10–12] and a large spin dependence of the current-voltage characteristics for the tunneling electrons through helical molecules [13–15]. Even enantio-separation and asymmetric electrochemical reactions by magnetic electrodes are reported [16, 17]. Furthermore, generation of large spin current was established for the inorganic chiral crystals [18–20]. These phenomena originated from the structural chirality is collectively termed as the chirality-induced spin selectivity (CISS) [21–23], where the spin is oriented parallel or antiparallel to the velocity of an injected electron depending on the materials' handedness.

CISS has been actively studied and become an interdisciplinary research fields spanning physics, chemistry, and biology. The reported spin-polarization up to 60 % amounts to the effective magnetic field of an order of 100 T [21], which is unrealistically strong. So far, several attempts have been made on the electron motion in a chiral molecule in the presence of spin-orbit coupling (SOC) [24–26]. The present status of theoretical studies is well summarized in Ref. [27]. In order to find an alternative explanation, we would like to understand the fact that CISS effect is observed even in the organic molecules with weak SOC strength in a way that do not rely explicitly on the strength of the SOC. Our belief here is based on the importance of interplay between nuclear and electronic motions which are governed by the same symmetry restrictions in chiral materials. Moreover, our objective also lies on a quest for CISS theory that do not violate the time reversal symmetry.

This is exactly what we address in this Letter.

To this end, we consider a molecule under the pseudo Jahn-Teller effect [28, 29], where the coupling between an electronic translation and rotation are mediated by the nuclear vibrational degrees of freedom. The Hamiltonian that includes the electron-nuclear coupling and the SOC satisfies the time-reversal symmetry. This symmetry confirms that the up-spin and the down-spin states are degenerate forming a Kramers pair. This degenerate pair can be separated from each other by its translational direction, which is made possible by the pseudo Jahn-Teller coupling. Consequently, the chiral molecule acts as the spin-filter by selecting the direction of electron translation. In this Letter, we will demonstrate that the performance of this chiral spin-filter is determined critically by the spin-selective transmission probability. In this model, angular momentum (AM) quantum numbers play crucial role in obtaining quite large efficiency insensitive to the SOC strength.

Molecular Basis. Molecular symmetry shapes a potential field that exerts on an electron injected into the molecule to create a rotational motion from the translational one. As a result, molecular orbital occupied by the injected electron is spanned by both translational and rotational basis. This study focuses on the point group C_3 as the minimal point group that allows chiral structure and has rotational basis with the one rotating in a direction opposite to the other. Let z -axis be the three-fold rotation axis. We write $|\phi_z\rangle$ for the translational state that are transformed as z , and $|\bar{\phi}_z\rangle := \Theta |\phi_z\rangle$ for its time-reversal with Θ being the time-reversal operator. Inclusion of $|\bar{\phi}_z\rangle$ allows us to construct the model Hamiltonian that satisfy the time-reversal symmetry in an unambiguous way. Obviously, $\langle \phi_z | \hat{p}_z | \phi_z \rangle = -\langle \bar{\phi}_z | \hat{p}_z | \bar{\phi}_z \rangle$ holds, where \hat{p}_z is the z -component of the electron momentum operator, and $\langle \phi_z | \hat{p}_z | \phi_z \rangle > 0$ is assumed. Because these basis belong to the A irreducible representation of the point group C_3 , they are

invariant under the three-fold rotation C_3 . The basis for the rotation on the xy -plane, which belong to the E_1 and E_2 irreducible representations, are denoted by $|\phi_{\pm}\rangle$. These rotational states are transformed under C_3 and Θ as

$$C_3 |\phi_{\pm}\rangle = e^{\mp i2\pi/3} |\phi_{\pm}\rangle, \quad (1)$$

and

$$\Theta |\phi_{\pm}\rangle = |\phi_{\mp}\rangle, \quad (2)$$

respectively.

In chiral materials, translational and rotational motions are coupled with each other [1]. However, in our model, the coupling between the translational and rotational states of an electron is mediated by the nuclear vibrational modes belonging to the e_1 and e_2 representation. Indeed, the product representation $e_i \times E_i$ for $i = 1, 2$ includes A representation. Consequently, there arises a finite matrix element $\langle A | e_i | E_i \rangle$ in a symbolic form. The nuclei in the $e_{1,2}$ representation also induce the coupling between the rotational states. This coupling between degenerate rotational states causes the spontaneous distortion, which is known as the Jahn-Teller effect [28, 29]. The coupling between non-degenerate (E_i and A) states, can also cause a similar symmetry-breaking called the pseudo Jahn-Teller effect [28, 29]. The nuclear coordinates in the $e_{1,2}$ representation are written as $Q_{\pm} = \rho e^{\pm i\varphi}$ with the radius ρ and the angle φ . The symmetry operations transform Q_{\pm} in the following way:

$$C_3 Q_{\pm} = e^{\pm i2\pi/3} Q_{\pm}, \quad (3)$$

and

$$\Theta Q_{\pm} = Q_{\mp}. \quad (4)$$

To describe the spin-dependent process, the electronic spin must be added to the basis. Let $|\uparrow\rangle$ and $|\downarrow\rangle$ denote the up-spin and down-spin states, respectively. They are transformed under the symmetry operations as

$$C_3 |\uparrow/\downarrow\rangle = e^{\mp i\pi/3} |\uparrow/\downarrow\rangle, \quad (5)$$

and

$$\Theta |\uparrow/\downarrow\rangle = \pm |\downarrow/\uparrow\rangle. \quad (6)$$

Model Hamiltonian. The Hamiltonian, H , describing an electron propagating through the chiral molecule consists of the electronic H_e , the nuclear H_n , the electron-nuclear coupling H_{en} Hamiltonians, which are all spin-independent, and the SOC Hamiltonian H_{soc} , $H = H_e + H_n + H_{en} + H_{soc}$. The electronic Hamiltonian is given by

$$H_e = \epsilon_{tr} (|\phi_z\rangle\langle\phi_z| + |\bar{\phi}_z\rangle\langle\bar{\phi}_z|) + \epsilon_{rot} (|\phi_+\rangle\langle\phi_+| + |\phi_-\rangle\langle\phi_-|), \quad (7)$$

where we set $\epsilon_{rot} \equiv 0$ throughout the paper, and the nuclear Hamiltonian is described as the two-dimensional harmonic oscillator,

$$H_n = -\frac{\hbar^2}{2M} \left(\frac{1}{\rho} \frac{\partial}{\partial \rho} \rho \frac{\partial}{\partial \rho} + \frac{1}{\rho^2} \frac{\partial^2}{\partial \varphi^2} \right) + \frac{M\omega^2}{2} \rho^2, \quad (8)$$

where M and ω are the nuclear mass and frequency, and \hbar is the Planck's constant. For derivation of H_{en} , we use the symmetry conditions $[H_{en}, C_3] = [H_{en}, \Theta] = 0$, and take only the first order in Q_{\pm} , which becomes (see Refs. [30] and Supplemental Material for details)

$$\begin{aligned} H_{en} = & V_+ Q_- |\phi_z\rangle\langle\phi_+| + V_- Q_+ |\phi_z\rangle\langle\phi_-| \\ & + V_-^* Q_- |\bar{\phi}_z\rangle\langle\phi_+| + V_+^* Q_+ |\bar{\phi}_z\rangle\langle\phi_-| \\ & + V_0 Q_- |\phi_+\rangle\langle\phi_-| + \text{H.c.}, \end{aligned} \quad (9)$$

where H.c. stands for the Hermite conjugate of all the preceding terms. The first and second lines of the right-hand-side of Eq. (9) represent the translation-rotation coupling with its strength V_{\pm} and the third line represents the rotation-rotation coupling with the coupling strength V_0 . Without loss of generality, these coupling constants can be always set to be real.

Here, we stress that the chirality imposes

$$V_+ \neq V_-. \quad (10)$$

Actually, the reflection symmetry leads to $V_+ \equiv V_-$. We see this by adding a vertical mirror, i.e., consider the case of the point group C_{3v} . In this case, the reflection operator σ_v acts on the molecular basis as $\sigma_v |\phi_{\pm}\rangle = |\phi_{\mp}\rangle$, $\sigma_v Q_{\pm} = Q_{\mp}$, and $\sigma_v |\uparrow/\downarrow\rangle = \pm |\downarrow/\uparrow\rangle$.

The only ingredient for the spin-dependent process in our model is the SOC. The derivation of H_{soc} is similar to that of H_{en} (see Ref. [31] and Supplemental Material for details): We use the symmetry conditions $[H_{soc}, K] = 0$ for $K = C_3, \sigma_v, \Theta$. Note that in this Letter, the only source of the chirality is the inequality of Eq. (10) and we impose the reflection symmetry on the SOC. For simplicity, we retain only the zeroth-order terms in Q_{\pm} ,

$$H_{soc} = \lambda (|\phi_+\rangle\langle\phi_+| - |\phi_-\rangle\langle\phi_-|) \otimes \hat{\sigma}_z, \quad (11)$$

with $\hat{\sigma}_z = |\uparrow\rangle\langle\uparrow| - |\downarrow\rangle\langle\downarrow|$ and the SOC strength λ . Eq. (11) indicates that spin-momentum locking works in the chiral molecule: In the cases of $V_+ > V_-$ and $V_+ < V_-$, the electron propagated with the positive momentum stabilizes the counter-clockwise ($|\phi_+\rangle$) and clockwise ($|\phi_-\rangle$) rotations, respectively. For $\lambda > 0$, this counterclockwise (clockwise) rotation stabilizes the down-spin (up-spin) state.

Observables. To numerically solve the Schrödinger equation for H , we need the nuclear eigenstates $\{|n, m\rangle\}$ to evaluate the matrix elements of H [32, 33]. Then, the product state comprised of the chiral molecule and injected electron is written as $|\Psi\rangle = \sum_{a=z, \bar{z}, +, -} \sum_{s=\uparrow, \downarrow} \sum_{n, m} C_{n, m}^{(a, s)} |\phi_a, s\rangle |n, m\rangle$ with $C_{n, m}^{(a, s)}$ being the coupling coefficient ($\phi_{\bar{z}} \equiv \bar{\phi}_z$ is used for convenience). The electron linear momentum and nuclear AM of $|\Psi\rangle$, which is analyzed later, are calculated from $P = \langle \Psi | \hat{p}_z | \Psi \rangle = g \langle \phi_z | \hat{p}_z | \phi_z \rangle$, where the momentum factor $g = \sum_{s, n, m} [|C_{n, m}^{(z, s)}|^2 - |C_{n, m}^{(\bar{z}, s)}|^2]$, and $L_n = \langle \Psi | (-i\hbar\partial_{\varphi}) | \Psi \rangle = \sum_{a, s, n, m} m\hbar |C_{n, m}^{(a, s)}|^2$, respectively [34]. Hereafter, the parameter values for the energy and coupling constants are given in units of $\hbar\omega$ and $(M\omega/\hbar)^{1/2}$, respectively.

Spin Selective Filtering Effect. The absence of the spin-flipping components in H_{soc} indicates that the injected electron pass through the molecule without changing its spin. This enables us to propose that the chiral molecule can act as the spin-filter: Suppose that a ground state $|\Psi\rangle$ has the positive momentum, $P = \langle \Psi | \hat{p}_z | \Psi \rangle > 0$, and the down-spin. Due to the time-reversal invariance of H , $\Theta |\Psi\rangle$ is degenerate with $|\Psi\rangle$, but has the negative momentum and the up-spin. Thus, these states form Kramers pair. In injecting a down-spin electron with $P > 0$ into the molecule, the electron propagates in accordance with $|\Psi\rangle$, the lowest state among eigenstates with the down-spin, to succeed in passing through the molecule because of the positivity of the momentum. In contrast, the injected up-spin electron with positive P propagates in accordance with $\Theta |\Psi\rangle$ and not with $|\Psi\rangle$ due to the mismatch of the spin. However, because the momentum of $\Theta |\Psi\rangle$ is negative, the up-spin electron cannot pass through the molecule (see Fig. 1(a) for the schematic picture). Therefore, the spin is selectively filtered depending on the translational direction of the lowest eigenstate among with the same spin as the injected one. It is of particular importance that this mechanism of the selective spin filtering requires the molecule to be chiral. Achiral molecule with $V_+ = V_-$ has the Hamiltonian invariant under the exchange of $|\phi_z\rangle$ and $|\bar{\phi}_z\rangle$, physically corresponding to the z -inversion invariance of the system. This invariance causes the disappearance of the momentum, $\langle \Psi | \hat{p}_z | \Psi \rangle \equiv 0$, which means that achiral molecules cannot utilize the translational direction of each eigenstate to filter the electronic spins. Therefore, the spin-filtering is the chirality-induced effect. Note that this filtering effect efficiently works only when the lowest state for the down-spin propagating in the positive translational direction is energetically well-separated from that for the up-spin. We call their energy difference as the spin barrier difference (SBD) denoted by δ , and explore the condition that the SBD becomes large enough to explain CISS not relying on the SOC strength λ .

In what follows, we consider the chiral case only, and without loss of generality, $V_+ > V_- > 0$ is assumed.

Classification of Eigenstates by AM Quantum Number. The fact that C_3 commutes with H allows us to classify all the energy eigenstates by their AM quantum number J . We write $|\Psi_J\rangle$ for the energy eigenstate with the AM quantum number J , which satisfies the eigenvalue equations $H |\Psi_J\rangle = E_J |\Psi_J\rangle$ and $C_3 |\Psi_J\rangle = e^{-i2\pi J/3} |\Psi_J\rangle$ with $J = 0, \pm 1$ for the spinless systems and $J = \pm 1/2, 3/2$ for the spinful systems. Note that J is determined up to the integer multiple of 3, and thus, $J = -3/2$ is equivalent with $J = 3/2$. From the time-reversal invariance, $|\Psi_J\rangle$ and $|\Psi_{-J}\rangle$ are degenerate, but with the opposite momentum and spin from each other, immediately leading to $\langle \Psi_0 | \hat{p}_z | \Psi_0 \rangle = 0$.

Now, we consider the effect of small but finite λ on the eigenstates. For distinction, we use a capital J and small letters j for the quantum number in the spinful and spinless systems, respectively, and corresponding state, energy, and momentum are denoted by $|\Psi_J\rangle$, E_J , and P_J for the spinful systems and $|\psi_j\rangle$, ϵ_j , and p_j for the spinless systems, respectively. Two

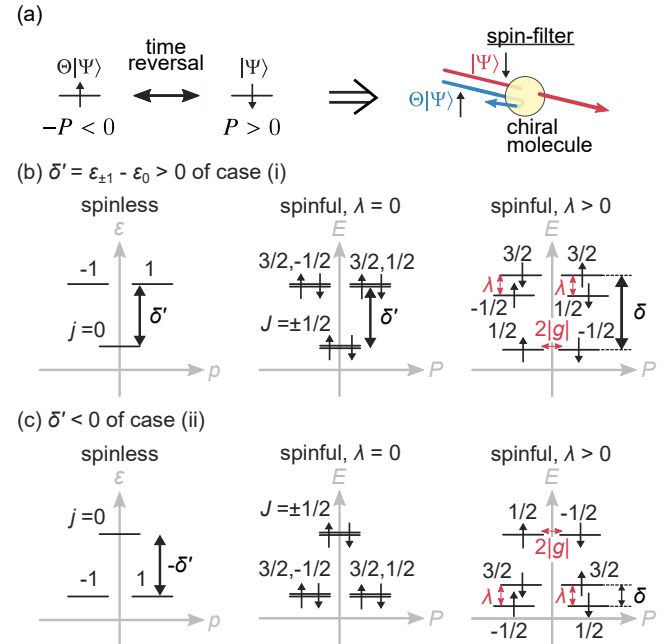


FIG. 1. (a) Schematic picture for the spin-filter of chiral molecules. (b), (c) Energy-Momentum diagrams of spinless, spinful with $\lambda = 0$, and spinful with $\lambda > 0$ systems for (b) $\delta' = \epsilon_{\pm 1} - \epsilon_0 > 0$ of case(i) and (c) $\delta' < 0$ of case(ii). Up-arrows and down-arrows represent the up-spin and down-spin, respectively.

quantum numbers are related by $J = j + 1/2$ for a up-spin and $J = j - 1/2$ for a down-spin. In the cases of $\lambda = 0$, the spinful states are given by $|\Psi_{j+1/2}\rangle \equiv |\psi_j\rangle |\uparrow\rangle$ or $|\Psi_{j-1/2}\rangle \equiv |\psi_j\rangle |\downarrow\rangle$, where the spatial part of the states is exactly the spinless state $|\psi_j\rangle$, indicating that $E_{j\pm 1/2} \equiv \epsilon_j$ and $P_{j\pm 1/2} \equiv p_j$. In contrast, in the cases of $\lambda > 0$, where the spatial part of $|\Psi_{j\pm 1/2}\rangle$ is modified from $|\psi_j\rangle$, these state have the different energy and momentum; For $j = 0$, the states with $J = \pm 1/2$ are degenerate (interchanged by the time-reversal operation) and $P_{\pm 1/2} \neq 0$ due to finite λ , as seen in Fig. 2(a), where the momentum factor g scales linearly with λ . The spin direction of the state is governed by the spin-momentum locking. For $\lambda > 0$ and $V_+ > V_-$, the momentum of the down-spin, namely, the state with $J = -1/2$, is positive. For $j = 1$ with $p_1 = -p_{-1} > 0$ in the cases of $V_+ > V_-$, the spin-momentum locking stabilizes the down-spin state, namely, $E_{3/2} > E_{1/2}$. The origin of the energy splitting in these states is the SOC.

SBD. Based on the above argument, we examine the SBD in the cases of (i) $\delta' := \epsilon_1 - \epsilon_0 > 0$ and (ii) $\delta' < 0$. In the case (i) (see Fig. 1(b) for the schematic picture), the chiral molecule filters the spin with the ground states $|\Psi_{0\pm 1/2}\rangle$. The SBD is, then, given by $\delta \equiv E_{3/2} - E_{-1/2} = \delta' + O(\lambda)$. Hence, under the condition that δ' is much larger than the contribution from the SOC, the SBD is approximated as $\delta \approx \delta'$, and can be nearly independent of λ , as numerically shown in Fig. 2(b). This condition will be discussed later. We propose that the efficient spin-filtering effect exactly corresponds to this situation, where the effect is insensitive to the magnitude of λ . On the other

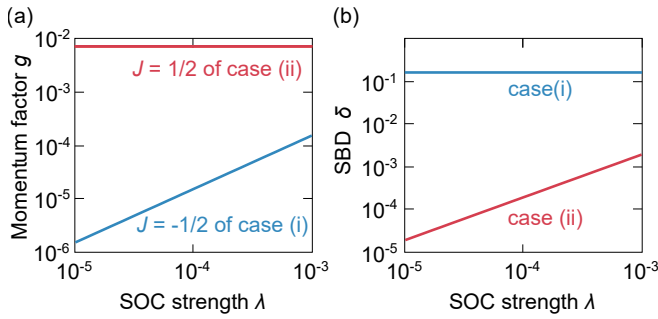


FIG. 2. (a) Momentum factor g of the ground state for the case (i) and (ii) are plotted as a function of the SOC strength λ . Momentum scales linearly for the case (i), whereas it is nearly independent of λ for the case (ii). (b) The SBD $\delta \equiv E_{3/2} - E_{-1/2}$ for the case (i) and $\delta \equiv E_{3/2} - E_{1/2}$ for the case (ii) are plotted as a function of λ .

hand, in the case (ii) (see Fig. 1(c) for the schematic picture), the spin-filtering occurs in the ground states $|\Psi_{1/2=1-1/2}\rangle$ and $|\Psi_{-1/2=-1+1/2}\rangle$. The SBD is then identical to $\delta \equiv E_{3/2} - E_{1/2} = O(\lambda)$, which is the energy difference caused by the SOC and thus scales linearly with λ as presented in Fig. 2(b). Therefore, the resultant spin filter efficiency is expected to be small.

Ground-State of Spinless Systems. We justify the conditions, under which the case (i) (Fig. 1(b)) holds, namely, $|\psi_0\rangle$ becomes the ground state for the spinless systems. We start this by presenting two limits that we can analytically identify the AM quantum number of the ground state. The first is the limit of $V_0 \equiv 0$, where the coupling between the rotational states disappears and only the translation-rotation coupling exist. In this limit, $\hat{l}_1 = -i\hbar\partial_\varphi - \hbar(|\phi_+\rangle\langle\phi_+| - |\phi_-\rangle\langle\phi_-|)$ is conserved with the integer eigenvalue $l_1/\hbar \in \mathbb{Z}$. Among them, the ground state is the state with $l_1 = 0$ that is simultaneously the eigenstate of C_3 with $j = 0$ [35]. Hence, the ground state is given by $|\psi_0\rangle$ in this limit. The second is the limit of $V_\pm \rightarrow 0$, where the translation and rotation are decoupled, which means that the injected electron directly pass through or is simply circulating in the molecule. In this limit, $\hat{l}_2 = -i\hbar\partial_\varphi + (\hbar/2)(|\phi_+\rangle\langle\phi_+| - |\phi_-\rangle\langle\phi_-|)$ is conserved with the half odd integer eigenvalue $l_2/\hbar = \pm(2n - 1)/2$ with $n \in \mathbb{N}$. The ground states are given by the state with $l_2/\hbar = \pm 1/2$ that are simultaneously the eigenstates of C_3 with $j = \pm 1$. Therefore, in this limit, $|\psi_{\pm 1}\rangle$ is the ground state.

General situations are located in between these two limits and the ground states are interchanged depending on the parameter values of ϵ_{tr} , V_\pm , and V_0 . Figure 3(a) presents the energy difference δ' as a function of the rotational coupling constant V_0 . As V_0 is decreased below 0.5, in which the situation approaches the first limit, δ' increases, thus strongly stabilizing the ground state with $j = 0$. Decreasing ϵ_{tr} and/or increasing V_\pm also make the system approach the first limit, in which the translation and rotation is strongly coupled. Therefore, the ground state is again given by $|\psi_0\rangle$, which is consistent with the numerical result presented in Fig. 3(b).

Finally, we mention that the energy difference δ' is cor-

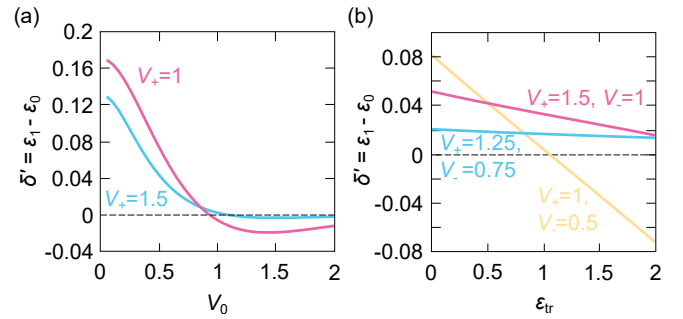


FIG. 3. (a) The energy differences of the spinless system $\epsilon_1 - \epsilon_0$ are plotted as a function of V_0 for $V_+ = 1$ and $V_+ = 1.5$ with fixed $V_- = 0.5$ and $\Delta = 0.1$. (b) The energy differences of the spinless system $\epsilon_1 - \epsilon_0$ are plotted as a function of ϵ_{tr} for various values of V_\pm with fixed $V_0 = 0.5$.

related with that of the nuclear AM. Figure 4(a) and (b) present the energy difference $\delta' = \epsilon_1 - \epsilon_0$ and the nuclear AM, $L_n = \langle\psi_1|(-i\hbar\partial_\varphi)|\psi_1\rangle$, respectively, as a function of $\Delta_V := V_+ - V_-$ with fixed V_+ . The behavior in Figs. 4(a) and (b) can be accounted for by an interplay between the nuclear rotational energy and the pseudo Jahn-Teller effect. In the $\Delta_V < 0.5$ region in Fig. 4(a), as Δ_V increases, this imbalance increases the nuclear AM and more differentiates $|\psi_{\pm 1}\rangle$ from $|\psi_0\rangle$, thus increasing δ' . However, increasing Δ_V by decreasing V_- also diminishes the pseudo Jahn-Teller effect, making the nuclear stable configuration close to the high-symmetry point, $\rho \equiv 0$, and hence reducing the nuclear average radius (see Fig. 4(c)-(e)), which leads to the decrease of the nuclear AM and thus, the nuclear rotational energy. The resultant energy difference decreases as presented in the large Δ_V region ($\Delta_V > 1.2$) in Fig. 4(a). Therefore, the nuclear vibrations have the role of not only mediating the translation-rotation coupling, but also increasing the energy difference δ' , and consequently enhancing the spin-filtering efficiency.

Concluding Remarks. In this Letter, we have theoretically explored the mechanism of the spin-filtering effect of chiral molecules. For that purpose, we have constructed a model of the point-group C_3 that consists of the electronic translational and rotational states, which are coupled with each other by the pseudo Jahn-Teller effect, or being mediated by the nuclear vibrational degrees of freedom. The time-reversal symmetry of the Hamiltonian makes it possible to possess, in combination with the SOC, the spin-momentum locking to filter the injected spin depending on the translational direction. Only when the injected spin state matches the lowest eigenstate of the same translational direction, the electron can selectively pass through the molecule with the ground state energy. This also enables us to classify the molecular eigenstates by their AM quantum number. When the spinless system has the ground state with $j = 0$, the SBD that determines the spin-filter efficiency is nearly independent of the SOC strength, and thus, makes it possible for the chiral molecule to act as the efficient spin-filter protected by the energy for AM quantization. Here

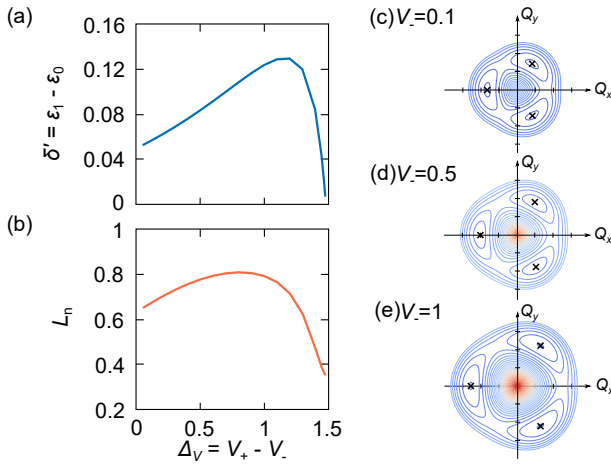


FIG. 4. (a) Energy difference $\delta' = \epsilon_1 - \epsilon_0$ and (b) nuclear AM L_n of $|\psi_1\rangle$ are plotted as a function of $\Delta V = V_+ - V_-$ with fixed V_+ . Other parameters are set to $\epsilon_{tr} = 0.1$ and $V_+ = 1.5$. (c)-(e) Ground state Born-Oppenheimer potential surfaces are depicted for $V_- = 0.1$ (c), 0.5 (d), and 1 (e). Crossed points display the location of the minimal points in each potential surface, which are farther from the origin as V_- increased.

we stress that δ' can be estimated at around 50 meV which is about twice as large as room temperature energy and is therefore enough to explain 60 % spin-polarization in the photoelectron spectroscopy. In the above estimate, as an example, we employed $\hbar\omega = 0.34$ eV (ca. 2740 cm^{-1}) in Ref. [36] and maximum reduced δ' value of 0.16 in Fig. 3 (a). The ground state with $j = 0$ for the spinless systems is obtained when the translation-rotation coupling constant V_\pm is sufficiently large compared to the rotational one V_0 . In our future work, the relation between the model parameters and the molecular structure should be clarified together with the direct estimation of the spin-filtering efficiency for actual chiral molecules. Additionally, the mechanism of the spin-filtering proposed in this Letter is not the specific property of the point-group C_3 , and will be straightforwardly generalized to other point or space groups to which many chiral and/or gyrotropic materials belong.

In this Letter, we have eliminated the spin-flipping components from the SOC, thus focusing only the spin-filtering effect and neglecting the spin-polarizing effect of chiral molecules. However, a chirality-induced bulk magnetization of CrNb_3S_6 seems to require the mechanisms that include the spin-polarizing effect [19]. Therefore, CISS seems to include both spin-filtering and spin-polarizing effects depending on the situations. In our model, as given explicitly in the Supplemental Material, we are also able to allow the nuclear-dependent SOC come into play, yielding the spin-flipping terms such as $(|\phi_+\rangle\langle\phi_+| - |\phi_-\rangle\langle\phi_-|) \otimes (Q_+\hat{\sigma}_+ + Q_-\hat{\sigma}_-)$ and $i(|\phi_z\rangle\langle\phi_z| - |\bar{\phi}_z\rangle\langle\bar{\phi}_z|) \otimes (Q_+\hat{\sigma}_+ - Q_-\hat{\sigma}_-)$ with $\hat{\sigma}_+ = |\uparrow\rangle\langle\downarrow|$ and $\hat{\sigma}_- = |\downarrow\rangle\langle\uparrow|$. These terms allow AM transfer from nuclear phonon to electron spin, thus polarizing the spin in the chiral molecule while respecting the conservation of AM. This AM conversion may be further enhanced when the molecule in-

volves conical intersections on the adiabatic potential energy surfaces [37, 38]. We here note that the current-induced magnetization phenomena, called the Edelstein effect, is apparently similar to the CISS effect from a global symmetry viewpoint. This effect is, however, interpreted as being mainly dominated by orbital effects [39, 40] and the resultant magnetization is much weaker than huge polarization caused by the CISS effect. The relevance of the spin-flipping components of the SOC to the spin-polarizing effect will be focused on in future studies.

We thank A. S. Ovchinnikov and I. G. Bostrem for discussions in the early stage of this work. This work was supported by the JSPS KAKENHI Grant No. 19H00891, No. 20J01875, and No. 21H01032.

- [1] L. D. Barron, *Molecular Light Scattering and Optical Activity*, 2nd ed. (Cambridge, 2004).
- [2] S. Mühlbauer, B. Binz, F. Jonietz, C. Pfleiderer, A. Rosch, A. Neubauer, R. Georgii, and P. Böni, Skyrmion Lattice in a Chiral Magnet, *Science* **323**, 915 (2009).
- [3] Y. Togawa, Y. Kousaka, K. Inoue, and J.-i. Kishine, Symmetry, Structure, and Dynamics of Monoaxial Chiral Magnets, *J. Phys. Soc. Jpn.* **85**, 112001 (2016).
- [4] L. Zhang and Q. Niu, Chiral Phonons at High-Symmetry Points in Monolayer Hexagonal Lattices, *Phys. Rev. Lett.* **115**, 115502 (2015).
- [5] H. Zhu, J. Yi, M.-Y. Li, J. Xiao, L. Zhang, C.-W. Yang, R. A. Kandl, L.-J. Li, Y. Wang, and X. Zhang, Observation of chiral phonons, *Science* **359**, 579 (2018).
- [6] J. Kishine, A. S. Ovchinnikov, and A. A. Tereshchenko, Chirality-Induced Phonon Dispersion in a Noncentrosymmetric Micropolar Crystal, *Phys. Rev. Lett.* **125**, 245302 (2020).
- [7] M. Kuwata-Gonokami, N. Saito, Y. Ino, M. Kauranen, K. Jefimovs, T. Vallius, J. Turunen, and Y. Svirko, Giant Optical Activity in Quasi-Two-Dimensional Planar Nanostructures, *Phys. Rev. Lett.* **95**, 227401 (2005).
- [8] G. L. J. A. Rikken, C. Strohm, and P. Wyder, Observation of Magnetoelectric Directional Anisotropy, *Phys. Rev. Lett.* **89**, 133005 (2002).
- [9] Y. Tokura and N. Nagaosa, Nonreciprocal responses from noncentrosymmetric quantum materials, *Nat. Commun.* **9**, 3740 (2018).
- [10] B. Göhler, V. Hamelbeck, T. Z. Markus, M. Kettner, G. F. Hanne, Z. Vager, R. Naaman, and H. Zacharias, Spin Selectivity in Electron Transmission Through Self-Assembled Monolayers of Double-Stranded DNA, *Science* **331**, 894 (2011).
- [11] D. Mishra, T. Z. Markus, R. Naaman, M. Kettner, B. Göhler, H. Zacharias, N. Friedman, M. Sheves, and C. Fontanesi, Spin-dependent electron transmission through bacteriorhodopsin embedded in purple membrane, *Proc. Natl. Acad. Sci.* **110**, 14872 (2013).
- [12] M. Kettner, B. Göhler, H. Zacharias, D. Mishra, V. Kiran, R. Naaman, C. Fontanesi, D. H. Waldeck, S. Sęk, J. Pawłowski, and J. Juhaniwicz, Spin Filtering in Electron Transport Through Chiral Oligopeptides, *J. Phys. Chem. C* **119**, 14542 (2015).
- [13] Z. Xie, T. Z. Markus, S. R. Cohen, Z. Vager, R. Gutierrez, and R. Naaman, Spin Specific Electron Conduction through DNA Oligomers, *Nano Lett.* **11**, 4652 (2011).
- [14] M. Kettner, V. V. Maslyuk, D. Nürenberg, J. Seibel, R. Gutierrez, G. Cuniberti, K.-H. Ernst, and H. Zacharias, Chirality-

Dependent Electron Spin Filtering by Molecular Monolayers of Helicenes, *J. Phys. Chem. Lett.* **9**, 2025 (2018).

[15] M. Suda, Y. Thathong, V. Promarak, H. Kojima, M. Nakamura, T. Shiraogawa, M. Ehara, and H. M. Yamamoto, Light-driven molecular switch for reconfigurable spin filters, *Nat. Commun.* **10**, 2455 (2019).

[16] K. Banerjee-Ghosh, O. Ben Dor, F. Tassinari, E. Capua, S. Yochelis, A. Capua, S.-H. Yang, S. S. P. Parkin, S. Sarkar, L. Kronik, L. T. Baczewski, R. Naaman, and Y. Paltiel, Separation of enantiomers by their enantiospecific interaction with achiral magnetic substrates, *Science* **360**, 1331 (2018).

[17] T. S. Metzger, S. Mishra, B. P. Bloom, N. Goren, A. Neubauer, G. Shmul, J. Wei, S. Yochelis, F. Tassinari, C. Fontanesi, D. H. Waldeck, Y. Paltiel, and R. Naaman, The Electron Spin as a Chiral Reagent, *Angew. Chem. Int. Ed.* **59**, 1653 (2020).

[18] A. Inui, R. Aoki, Y. Nishiue, K. Shiota, Y. Kousaka, H. Shishido, D. Hirobe, M. Suda, J.-i. Ohe, J.-i. Kishine, H. M. Yamamoto, and Y. Togawa, Chirality-Induced Spin-Polarized State of a Chiral Crystal CrNb_3S_6 , *Phys. Rev. Lett.* **124**, 166602 (2020).

[19] Y. Nabei, D. Hirobe, Y. Shimamoto, K. Shiota, A. Inui, Y. Kousaka, Y. Togawa, and H. M. Yamamoto, Current-induced bulk magnetization of a chiral crystal CrNb_3S_6 , *Appl. Phys. Lett.* **117**, 052408 (2020).

[20] K. Shiota, A. Inui, Y. Hosaka, R. Amano, Y. Ōnuki, M. Hedo, T. Nakama, D. Hirobe, J.-i. Ohe, J.-i. Kishine, H. M. Yamamoto, H. Shishido, and Y. Togawa, Chirality-Induced Spin Polarization over Macroscopic Distances in Chiral Disilicide Crystals, *Phys. Rev. Lett.* **127**, 126602 (2021).

[21] R. Naaman and D. H. Waldeck, Chiral-Induced Spin Selectivity Effect, *J. Phys. Chem. Lett.* **3**, 2178 (2012).

[22] R. Naaman, Y. Paltiel, and D. H. Waldeck, Chiral molecules and the electron spin, *Nat. Rev. Chem.* **3**, 250 (2019).

[23] R. Naaman, Y. Paltiel, and D. H. Waldeck, Chiral Molecules and the Spin Selectivity Effect, *J. Phys. Chem. Lett.* **11**, 3660 (2020).

[24] A.-M. Guo and Q.-f. Sun, Spin-Selective Transport of Electrons in DNA Double Helix, *Phys. Rev. Lett.* **108**, 218102 (2012).

[25] A.-M. Guo and Q.-F. Sun, Spin-dependent electron transport in protein-like single-helical molecules, *Proc. Natl. Acad. Sci.* **111**, 11658 (2014).

[26] S. Matityahu, Y. Utsumi, A. Aharony, O. Entin-Wohlman, and C. A. Balseiro, Spin-dependent transport through a chiral molecule in the presence of spin-orbit interaction and nonunitary effects, *Phys. Rev. B* **93**, 075407 (2016).

[27] F. Evers, A. Aharony, N. Bar-Gill, O. Entin-Wohlman, P. Hedegård, O. Hod, P. Jelinek, G. Kamieniarz, M. Lemeshko, K. Michaeli, V. Mujica, R. Naaman, Y. Paltiel, S. Refaelly-Abramson, O. Tal, J. Thijssen, M. Thoss, J. M. van Ruitenbeek, L. Venkataraman, D. H. Waldeck, B. Yan, and L. Kronik, Theory of Chirality Induced Spin Selectivity: Progress and Challenges, *arXiv:2108.09998 [cond-mat]* (2021).

[28] I. Bersuker, *The Jahn-Teller Effect* (Cambridge, 2006).

[29] I. B. Bersuker, Jahn-Teller and Pseudo-Jahn-Teller Effects: From Particular Features to General Tools in Exploring Molecular and Solid State Properties, *Chem. Rev.* **121**, 1463 (2021).

[30] T. Zeng, R. J. Hickman, A. Kadri, and I. Seidu, General Formalism of Vibronic Hamiltonians for Tetrahedral and Octahedral Systems: Problems That Involve T , E States and t , e Vibrations, *J. Chem. Theory Comput.* **13**, 5004 (2017).

[31] K. Wang and T. Zeng, Hamiltonian formalism of spin-orbit Jahn-Teller and pseudo-Jahn-Teller problems in trigonal and tetragonal symmetries, *Phys. Chem. Chem. Phys.* **21**, 18939 (2019).

[32] H. Koizumi and S. Sugano, The geometric phase in two electronic level systems, *J. Chem. Phys.* **101**, 4903 (1994).

[33] R. Requist, F. Tandetzky, and E. K. U. Gross, Molecular geometric phase from the exact electron-nuclear factorization, *Phys. Rev. A* **93**, 042108 (2016).

[34] See Supplemental Material for technical details of the numerical calculation.

[35] See Supplemental Material for detailed discussion.

[36] P. B. Allen, A. G. Abanov, and R. Requist, Quantum electrical dipole in triangular systems: A model for spontaneous polarity in metal clusters, *Phys. Rev. A* **71**, 043203 (2005).

[37] Y. Wu and J. E. Subotnik, Electronic spin separation induced by nuclear motion near conical intersections, *Nat. Commun.* **12**, 700 (2021).

[38] X. Bian, Y. Wu, H.-H. Teh, Z. Zhou, H.-T. Chen, and J. E. Subotnik, Modeling nonadiabatic dynamics with degenerate electronic states, intersystem crossing, and spin separation: A key goal for chemical physics, *J. Chem. Phys.* **154**, 110901 (2021).

[39] T. Furukawa, Y. Shimokawa, K. Kobayashi, and T. Itou, Observation of current-induced bulk magnetization in elemental tellurium, *Nat. Commun.* **8**, 954 (2017).

[40] T. Yoda, T. Yokoyama, and S. Murakami, Orbital Edelstein effect as a condensed-matter analog of solenoids, *Nano Lett.* **18**, 916 (2018).